resources

MDPI

Article

Saving Raw Materials for Cement Manufacture and Reusing an Untreated Waste from the Petrochemical Industry

Bruno Sena da Fonseca [1], António Castela [2], Rui Neves [3,*], Raquel Duarte [3], Carlos Galhano [3,4] and Maria de Fátima Montemor [1]

1 Centro de Química Estrutural-CQE, IST, University of Lisbon, 1049-001 Lisbon, Portugal; bruno.fonseca@tecnico.ulisboa.pt (B.S.d.F.); mfmontemor@ist.utl.pt (M.d.F.M.)
2 Polytechnic Institute of Setúbal, Setúbal Technology School, 2914-761 Setúbal, Portugal; Antonio.Castela@estsetubal.ips.pt
3 Polytechnic Institute of Setúbal, Barreiro Technology School, 2839-001 Lavradio, Portugal; raquel.duarte@estbarreiro.ips.pt (R.D.); acag@fct.unl.pt (C.G.)
4 Faculdade de Ciências e Tecnologia, U.N.L., 2829-516 Caparica, Portugal
* Correspondence: rui.neves@estbarreiro.ips.pt

Received: 20 August 2018; Accepted: 11 September 2018; Published: 12 September 2018

Abstract: This research addresses the replacement of cement by an untreated waste from the petrochemical industry. The effects of partial replacement of cement by spent fluid cracking catalyst (SFCC) on properties of mortar were determined. In this study, a series of mortar mixes was prepared with replacement ratios of 0%, 3%, 6%, and 12%. Furthermore, performance enhancing factors such as SFCC treatment or use of plasticizers were avoided. Workability, compressive strength, and durability related properties were assessed. An improvement regarding resistance to chloride penetration was observed, as well as that, when curing in salt water, the use of SFCC may be advantageous regarding compressive strength.

Keywords: SFCC; mortar; curing; strength; durability

1. Introduction

Nowadays, the construction industry is making an effort to incorporate different types of waste into cementitious composites, contributing to sustainability through materials diversification, cost decrease, and judicious use of raw materials [1]. The CO_2 emissions, as well as the consumption of natural resources, associated to cement production encourage the use of industrial wastes as supplementary cementing materials (SCM). The petrochemical industry generates a by-product, a catalyst from the fluid catalytic cracking units, which after several cycles of use and regeneration becomes exhausted. These spent fluid cracking catalysts (SFCC) are aluminosilicates and thus can be used as binder in cementitious mixes [2]. The partial replacement of cement by SFCC brings three potential advantages: the diminution of CO_2 emissions, the saving of raw materials for cement production, and the reuse of a waste. Therefore, the SFCC influence on cementitious composites has been investigated.

Su et al. [3] experimentally investigated the toxicity of SFCC due to and eventual leaching of heavy metals and concluded that it is a non-hazardous material. Although it was found that SFCC diminishes workability [4,5] and carbonation resistance [6], while it improves the resistance to chloride penetration [7,8], the influence on compressive strength is not clear [9]. Moreover, results of SFCC influence on transport properties of cementitious composites are scarce. Serious deterioration problems such as sulphate attack and alkali-silica reaction involve the transport of the deleterious ions and

liquids through the porous structure of cementitious composites and therefore, testing transport processes—such as sorptivity and permeability—is crucial on the basis of durability assessment.

A standout fact in the literature review is the range of replacement ratio, with a maximum of 50% [10] and with an average around 15%. Considering the worldwide annual amount of generated SFCC—around 160 thousand tonnes [11]—and the current annual cement production/consumption of 4100 million tonnes [12], the above mentioned ratios will rapidly expend the whole of the generated SFCC. On the other hand, if limited amounts per application are allowed, the impact of SFCC incorporation may be low, even negligible.

Furthermore, most investigations have been carried out on treated, i.e., ground or thermally activated, SFCC, whereas an eco-friendly strategy shall aim at avoiding energy-consuming processes, such as those.

The aim of this study is to investigate the influence of low amounts of untreated, i.e., as disposed, SFCC as cement replacement in the properties of cement mortars, without changing the superplasticizer content. Moreover, as in the construction of some maritime structures' concrete, the cementitious composite is submerged in seawater just hours after casting, because this is a cheaper and easier curing process [13]; the influence of cement replacement by SFCC on compressive strength under such conditions is also addressed.

2. Materials and Methods

A series of tests was conducted, initially aiming at a comprehensive characterization of SFCC. Anticipating a loss of workability when replacing cement by untreated SFCC, and still envisaging to avoid the use of plasticizers, a high water-cement ratio was adopted. Thus, a mortar mix using cement, sand, and water in mass proportions of 1:3:0.60 was used as reference mortar. The remaining mixes were based on the previous one with cement replacement by SFCC at distinct levels: 3%, 6%, and 12% (mass). No chemical admixtures were added. The mix coding is defined following the replacement level: R0 (reference mix), R3, R6, and R12. All mixes were tested for workability, compressive strength (with different curing conditions), sorptivity, air-permeability, carbonation resistance, and resistance to chloride penetration.

2.1. Materials

The materials used in the present investigation included an ordinary Portland cement, conforming to EN 197-1 [14] requirements for CEM I 42.5R, SFCC powder, as mineral admixture, and a 0–4 mm siliceous natural sand. The SFCC powder was supplied by a cracking catalytic unit (Sines-Portugal refinery). It was tested and used as received. Table 1 provides the estimated chemical composition of SFCC and cement. The SFCC seems mainly composed of SiO_2 and Al_2O_3 and residual amounts of other species. Figure 1 reveals spherical/elliptic particles of SFCC and some clusters as well. These clusters were formed during the previous activity of the material as catalyst. Furthermore, the sequence and intensity of major peaks identified in the X-ray diffractogram (D8, Bruker, Billerica, MA, USA) (Figure 2) are typical from an original zeolite variety named faujasite [15].

Table 1. Estimated chemical composition in terms of oxides percentage.

Powder	SiO_2	Al_2O_3	Fe_2O_3	MgO	MnO	CaO	Na_2O	K_2O	SO_3	L.O.I. [1]
SFCC	44.62	49.01	1.42	0.04	1.30	0.58	0.06	0.45	0.53	2.26
Cement	19.56	4.23	3.12	1.30	- [2]	63.30	0.22	0.31	2.76	3.75

[1] Loss on ignition. [2] Not detected.

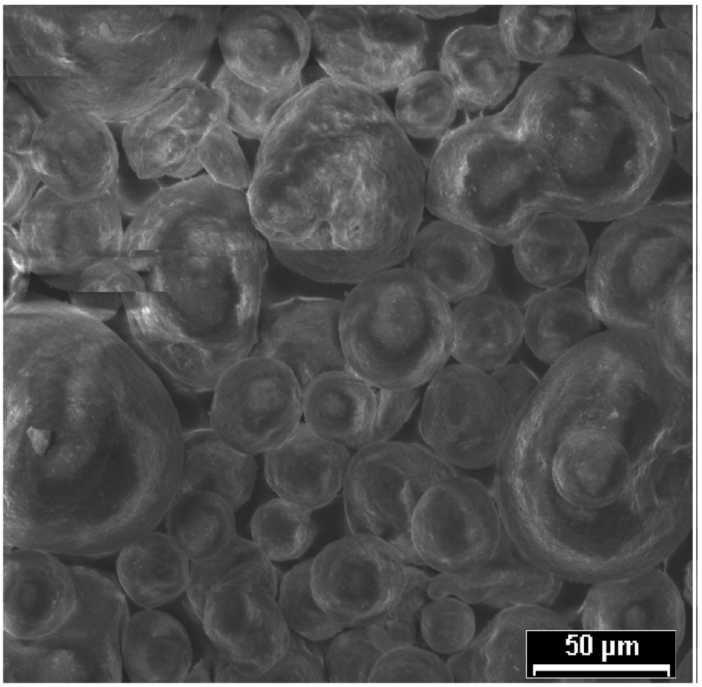

Figure 1. SEM image showing the morphology of the spent fluid cracking catalyst (SFCC) particles.

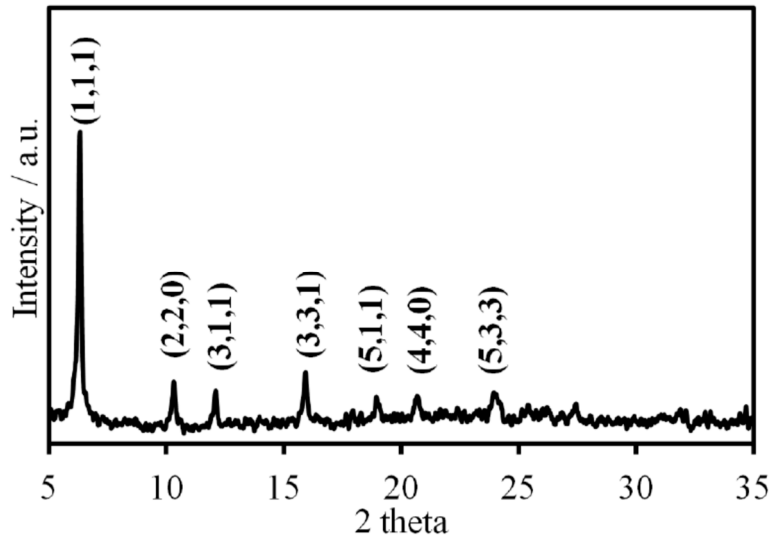

Figure 2. XRD pattern of the studied SFCC.

The specific surface areas of SFCC and cement are 118 m^2/g and 375 m^2/kg, as assessed through Brunauer-Emmett-Teller (BET) and Blaine methods, respectively, while the respective specific gravities are 2.17 g/cm^3 and 3.14 g/cm^3. The siliceous sand had a specific gravity of 2.63 g/cm^3. Figure 3 depicts the particle size distribution of each solid constituent of the mortar. The SFCC is mainly composed of particles with diameters between 20 and 500 µm, whereas the cement has particles with sizes ranging between 0.4 and 300 µm.

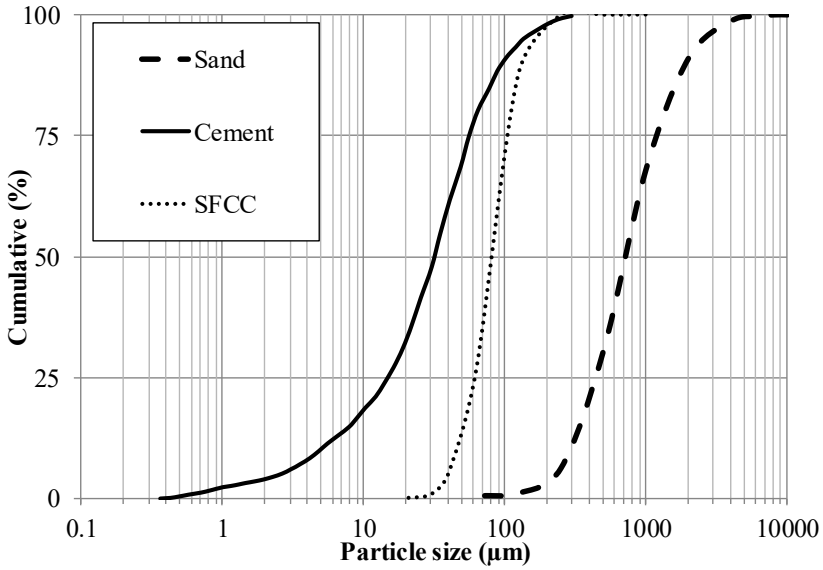

Figure 3. Particle size distribution of mortar constituents.

The evaluation of pozzolanic activity was performed using an indirect method: electrical conductivity variation. A 200 mL volume of saturated solution of $Ca(OH)_2$ was prepared and maintained under stirring at a temperature of 40 ± 1 °C while measurements of conductivity were made until a constant value was reached (≈7 mS/cm). Thereafter, 5 g of SFCC powder were added to the solution and the conductivity measurements continued for 60 min.

The conductivity evolution of the saturated lime solution after adding the SFCC is depicted in Figure 4. At the early stages, a significant decrease of the electrical conductivity of the suspension was observed. This behavior is explained by a decrease of $Ca(OH)_2$ concentration in solution due to the pozzolanic reactions. According to Lúxan et al. [16], the greater the reduction, the better the pozzolanic activity of the material, and if the conductivity decreases more than 1.20 mS/cm in the first 2 min, the material has good pozzolanic activity. The present SFCC showed a decrease of 2.21 mS/cm after 2 min.

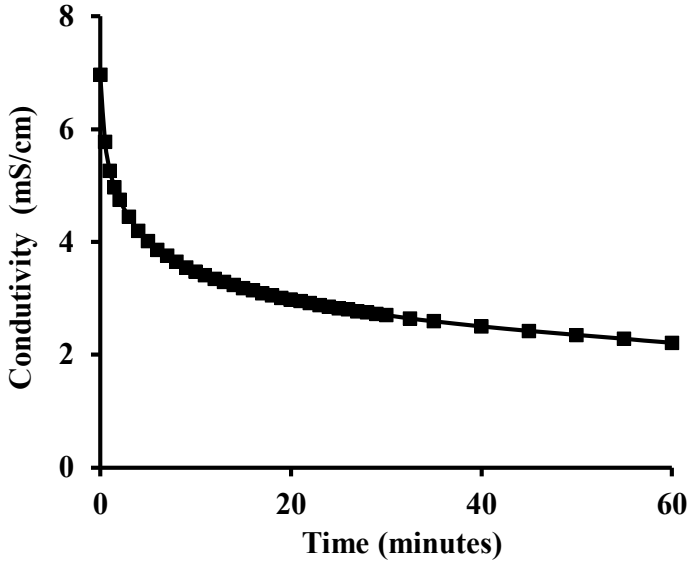

Figure 4. Evolution of lime solution conductivity after adding the SFCC powder.

2.2. Specimens Preparation

For each mortar mix, 40 × 40 × 160 mm prisms and cylinders with 150 mm diameter and 300 mm long were cast. All the specimens were cast in steel molds, compacted using a vibration table, and demolded at 24 h.

Twelve prisms were cured in salt water (3% NaCl solution) until the age of testing, another 12 prisms were cured in water, also until the age of testing. These specimens were destined for compressive strength testing. The remaining specimens, destined for durability testing, were cured in water for 7 days and then kept in a climate chamber at 20 °C and 65% RH until testing or until they went through a specific preparation when required. At the age of 7 days, the 300 mm long and 150 mm diameter specimens were sawn into slices of 50 mm.

2.3. Methods

2.3.1. Workability

The workability of fresh mortars was measured using the apparatus and following the test procedures defined in ASTM C1437-13 [17] and is indicated by the mean spread diameter of tested samples on the flow table.

A truncated conical mold was filled in two layers upon a circular table. After removing the mold, the specimen was spread by jolting the flow table 25 times at a constant rate, for 15 s. The diameter of the mortar was then measured in two directions, mutually perpendicular.

2.3.2. Compressive Strength

To investigate the influence of age and of the type of curing in the compressive strength of mortars modified with untreated SFCC, compression tests were carried out in a Matest cement compression machine, equipped with a load cell whose maximum capacity is 250 kN, at a load rate of 2400 N/s, as defined in EN 196-1 [18]. Each sample comprised at least 3 specimens. Compressive strength was assessed at 28 days, as it is a reference age for testing cementitious composites and at a later age (90 days) to allow further development of the pozzolanic reaction due to SFCC incorporation.

2.3.3. Sorptivity

The sorptivity test was performed following the basic procedures defined in ASTM C1585-13 [19], in 3 prismatic specimens of each mix, aged 54 days, whose long edge surfaces were sealed by means of an epoxy coating. A multi-layer of filter papers with an approximate thickness of 10 mm was placed inside a closed container. Then, water was added until the papers were soaked and was kept at a level adjacent to the top of the multi-layer. Three specimens of each mix were placed upon the multi-layer and, due to the deformation of the last, they got in contact with water. This setup allows a water intake due to capillary forces at the mortar pores. The amount of absorbed water was assessed by weighing the specimens at regular intervals: 1, 5, 10, 20, and 30 min; 1, 2, 3, 4, 5, 6, 7, 8, and 9 h; 1, 2, 3, 5, 6, 7, and 8 days. The coefficient of initial sorptivity (S_i) is estimated by linear regression as the positive slope of the water absorbed per unit area versus unit time within the first 24 h of testing. The second stage of sorptivity (S_s) corresponds to the second linear section of the curve and is estimated by linear regression from the points taken within the first and eighth days of testing.

2.3.4. Air-Permeability

Air-permeability was assessed using a test method that is considered in Swiss standard SN 505 206/1 [20]. An initial negative relative pressure is applied at specimen surface, through a test chamber. Afterwards, permeation causes a pressure variation in the test chamber. At the end of 12 min or the

time elapsed until a pressure change of 20 mbar is reached, whichever occurs first, data is recorded. Then, an air-permeability coefficient may be calculated using the following equation [21]:

$$kT = \left(\frac{V_c}{A}\right)^2 \times \frac{\mu}{2 \times \varepsilon \times p_a} \times \left(\frac{\ln\left(\frac{p_a+\Delta p}{p_a-\Delta p}\right)}{\sqrt{t_f} - \sqrt{t_i}}\right) \quad (1)$$

where kT is the air permeability coefficient (m^2), V_c is volume of test chamber (m^3), A is cross section of test chamber (m^2), μ is viscosity of air at 20 °C ($N{\cdot}s/m^2$), ε is porosity of the material (-), p_a is atmospheric pressure (N/m^2), Δp is pressure increase in test chamber (N/m^2), t_i is time at start of measurement (s), and t_f is time at end of measurement (s).

Six tests per mix were carried out, in mortar discs aged 56 days.

2.3.5. Carbonation Resistance

The carbonation resistance was assessed in accelerated conditions. Three prismatic specimens for each mix, aged 35 days, where two opposite long edge faces and the two minor faces were previously coated with a double layer of adhesive aluminium, were placed in a climate chamber at 20 °C, 65% RH, and with a CO_2 content of 5%, as suggested in the LNEC standard E 391 [22]. The specimens were removed from the chamber after an exposure period of 28 days, as suggested in Model Code for Service Life Design [23]. Afterwards, they were split, and the broken surfaces were immediately cleaned and then sprayed with a phenolphthalein colour indicator. The thickness where the indicator did not react corresponds to the carbonated region. The carbonation depth for each mix is given by the mean of the 24 thickness readings (8 readings per specimen).

2.3.6. Resistance to Chloride Penetration

The resistance to chloride penetration was assessed through an accelerated non-steady state migration test [24], using the rapid chloride permeability test setup [25], in mortar specimens with an age of 72 days. Migration allows a fast assessment of concrete ability to resist chloride penetration, as chloride ion ingress is accelerated by means of applying an electrical field across the specimens. In this study potentials up to 20 V were applied. Usually, higher voltages are applied but as in this experiment 150 mm diameter discs are used instead of the standard 100 mm, lower voltages are foreseen. The applied voltage, temperature of anodic solution, and test duration were recorded. At the end of the test, the chloride penetration depth was measured, by means of a colorimetric technique. A silver nitrate solution (0.1 M) was used as a colorimetric indicator, at broken surfaces of the tested specimens. Finally, non-steady-state diffusion coefficients were obtained, using Equation (2), based on the Nernst–Einstein equation [26].

$$D = \frac{R\ T\ L}{z\ F\ (U-2)} \times \left(\frac{x_d - \alpha\sqrt{x_d}}{t}\right) \quad (2)$$

where

$$\alpha = 2\sqrt{\frac{R\ T\ L}{z\ F\ (U-2)}} \times erf^{-1}\left(1 - 2\frac{c_d}{c_0}\right) \quad (3)$$

D is the non-steady-state diffusion coefficient (m^2/s), R the gas constant, (R = 8.314 J/(K·mol)), z the absolute value of ion valence, for chloride (z = 1), F the Faraday's constant ($F = 9.648 \times 10^4$ J/(V·mol)), T the average temperature during the test (K), L the thickness of the specimen (m), U the absolute value of applied voltage (V), x_d the average chloride penetration depth (m), t the test duration (s), erf^{-1} the inverse of error function, c_d the chloride concentration at which the color changes ($c_d \approx 0.07$ M, for ordinary Portland cement), and c_0 is the chloride concentration in the cathode (c_0 = 2 M).

3. Results and Discussion

3.1. Workability

Figure 5 depicts the workability results from the flow table test. A consistent decrease of flow table spread with increasing SFCC content is observed. Once the water-binder ratio was kept constant and no plasticizer was added, and while SFCC is a highly water demanding material [27–29], it is suggested that the flow table spread decreased because there was less available water to decrease friction between particles. Besides the water demanding characteristic, explained by the larger surface area of SFCC [30], the detected narrow size range of SFCC, in comparison with that of the replaced cement, also jeopardizes workability.

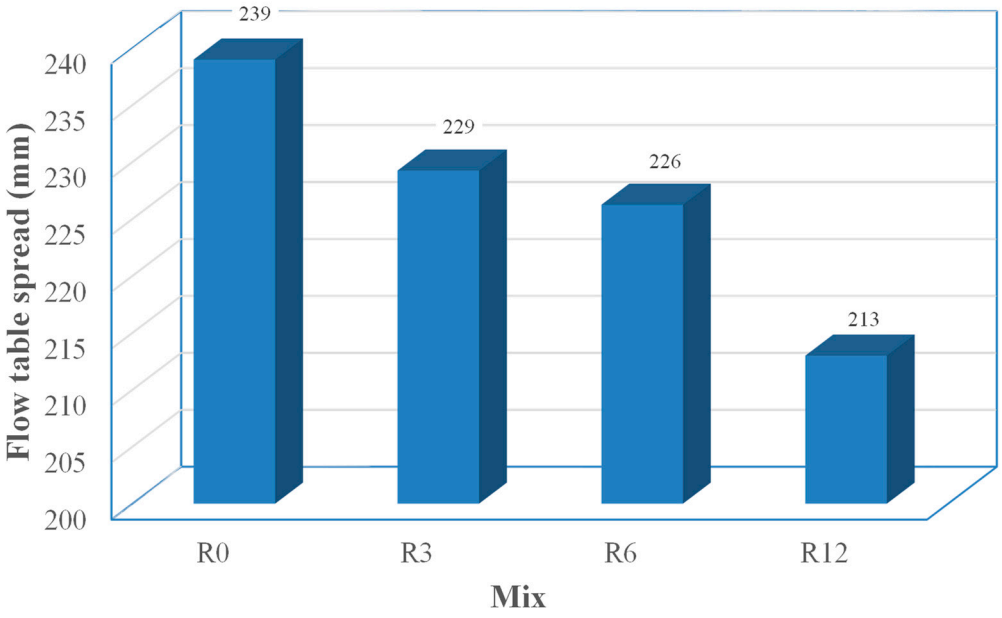

Figure 5. Workability obtained from flow table test.

3.2. Compressive Strength

The compressive strengths of the mortar mixes cured in tap water and in salt water are summarized in Tables 2 and 3. It can be noticed that increasing SFCC replacement levels lead to a slight but consistent compressive strength decrease in specimens cured in tap water. Such a trend is not detected in the results obtained in salt-water-cured specimens. In this case, the compressive strength results fluctuate, and similar values were obtained for the different mixes. Furthermore, the later testing age revealed slightly higher (around 10%) compressive strengths than at 28 days for all mixes, regardless of being cured in tap or salt water. There is also evidence that curing in salt water limits the compressive strength.

Although increases in compressive strength with the use of SFCC have been reported [31,32], in those investigations SFCC was either previously treated (ground), which improves its reactivity, or accompanied by an increase in the superplasticizer dosage. This was not the case in the present investigation. It also shall be mentioned that as the density of SFCC is lower than that of cement and as the mixes are designed in fixed mass proportions of binder-sand-water, when replacing cement by SFCC it corresponds to a slightly lower binder content per unit volume of mortar than in the reference mix.

The low relative increase in strength between 28 days and 90 days proves that SFCC has a short-term pozzolanic activity, as found by Zornoza et al. [29].

The mixes without SFCC, in both testing ages, showed lower compressive strength when cured in salt water than when cured in tap water. However, this effect was mitigated with SFCC addition.

In fact, sodium chloride acts as a setting and hardening accelerator, leading to higher compressive strength at 7 days and 14 days, due to the formation of Friedel's salt [33]. When setting accelerators are applied, the final strength (28 days and later ages) of the cement composite is expected to be limited [34]. This happened in this investigation and has parallels in other publications [35–38].

This investigation confirms, for the particular case of SFCC, the positive impact of pozzolanic additions in the compressive strength evolution with time in concrete mixes exposed to sea water that has been reported elsewhere [39,40]. The mitigation of strength loss for salt water curing may be justified by the increase in aluminates content brought by SFCC that, when combined with NaCl, minimizes the mentioned chloride effect on the strength limitation at 28 days and later testing ages. Another possible contributing factor may be the decrease of the portlandite content caused by SFCC, as portlandite is a leachable product by waters containing dissolved chlorides, which leads to strength losses in cementitious composites [34].

Table 2. Compressive strength of the mortar mixes cured in tap water.

Notation	SFCC (%)	Compressive Strength (MPa)	
		28-day	90-day
R0	0	49.7	53.9
R3	3	47.6	53.8
R6	6	46.5	51.6
R12	12	46.2	51.3

Table 3. Compressive strength of the mortar mixes cured in salt water.

Notation	SFCC (%)	Compressive Strength (MPa)	
		28-day	90-day
R0	0	44.5	49.8
R3	3	45.9	49.1
R6	6	43.8	49.3
R12	12	44.6	49.0

3.3. Sorptivity

Figure 6 shows the average water uptake by capillary action. As a linear variation of the amount of water absorbed by an ideal capillary with the square root of time is mathematically proved [41], these results are plotted as a function of the square root of time. The corresponding initial sorptivity (S_i) and secondary sorptivity (S_s) coefficients, computed through linear fitting of the capillary absorption results, within the first 24 h of testing and between the first and eighth days of testing, respectively, are shown in Figure 7. Although it is known that pozzolanic reactions promote the pore disconnection [42], providing reaction products that are very efficient in filling up capillary spaces thus improving the imperviousness of the system [43], there is a trend for the increase of S_i with the increase of SFCC replacement. This trend was also observed by Barbhuiya et al. [44] with a different SCM. This foresees an increase in capillary porosity that may be attributed to SFCC being a coarser and more uniform powder than cement [45] and to its high water absorption. This effect is less pronounced in the second stage sorptivity, as the maximum relative difference to R0 coefficients is 44% for S_i and is 19% for S_s.

Analyzing the results from the point of view of practical application, despite the high water-binder ratio (0.6), all mixes exhibit sorptivity values below 500 g/($m^2 \cdot h^{0.5}$), considered the threshold value in EN 1504-3 [46], the European standard which specifies the performance requirements for structural and non-structural repair products.

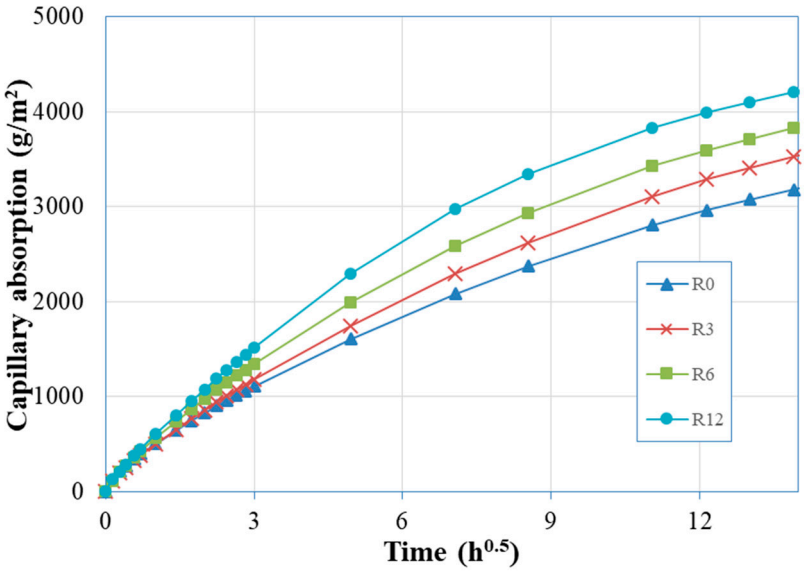

Figure 6. Capillary absorption.

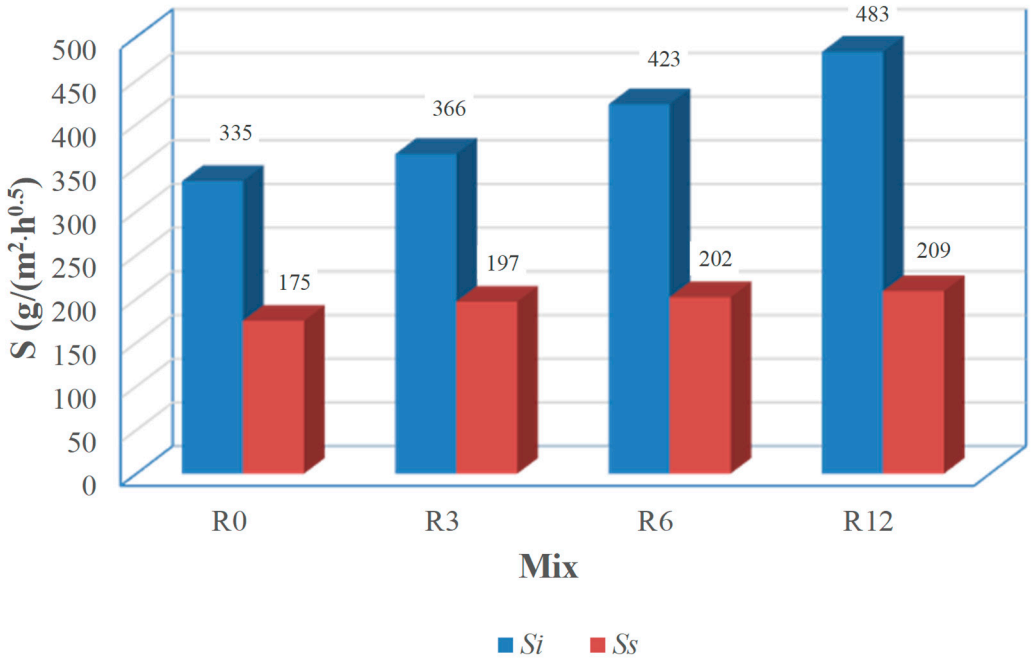

Figure 7. Sorptivity coefficients.

3.4. Air-Permeability

As gas-permeability results are known to have high scatter and outliers are likely to occur, the use of robust statistics is advised [47]. Thus, the results shown in Figure 8 represent the median of the values of each mix. A consistent increase in air-permeability with increasing replacement of cement by SFCC was obtained. Although a maximum relative increase of more than 100% is found, it must be mentioned that gas-permeability results are usually interpreted in a logarithmic basis, in which that maximum relative difference becomes 23%. The reasons behind this increase are believed to be those pointed to in the discussion of the sorptivity results (see Section 3.3). Actually, an interesting relationship between these transport properties is found, as depicted in Figure 9, where the correlation between air-permeability and S_i is higher than between air-permeability and S_s. Furthermore, a good correlation between air-permeability coefficient and 28-day compressive strength was also found (Figure 10). Again, from the point of view of practical application, and according to a quality classification of the

material based on this air-permeability coefficient, proposed by Torrent and Frenzer [48], all mixes are rated as of "very good" quality.

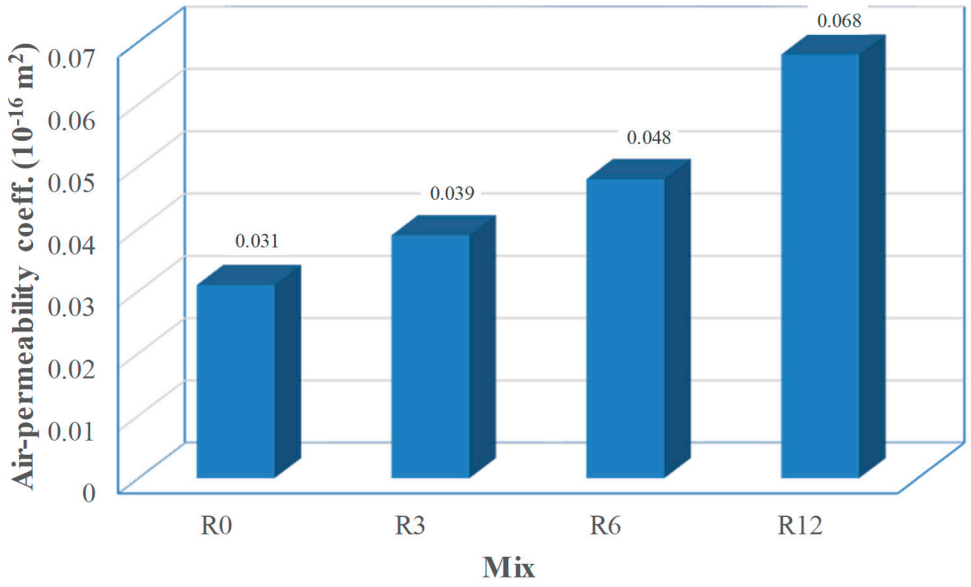

Figure 8. Air-permeability coefficients.

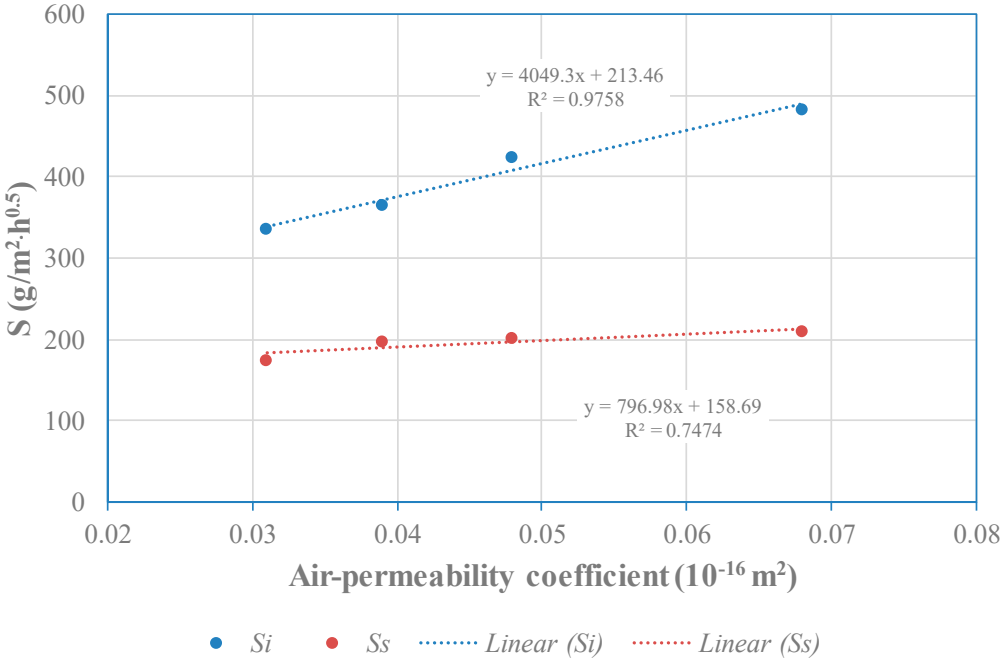

Figure 9. Relationship between sorptivity and air-permeability.

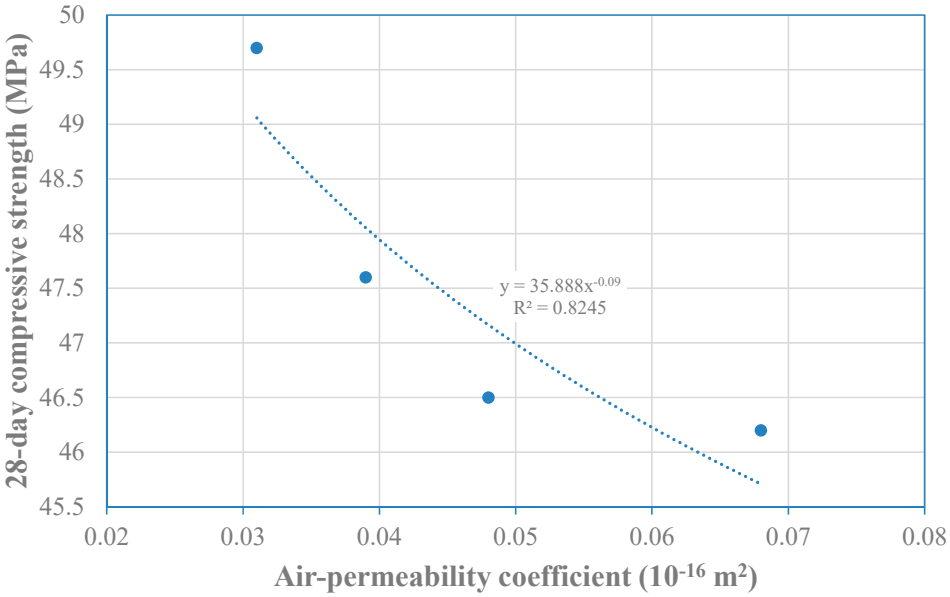

Figure 10. Relationship between 28-day compressive strength and air-permeability.

3.5. Carbonation Resistance

The mean carbonation depths of the tested mixes are depicted in Figure 11. The carbonation depth increased with the increasing level of cement replacement by SFCC. Thus, the maximum relative difference to the reference mix is obtained for mix R12 and it is 25%. However, Hilsdorf [49] found a linear relationship between the square of carbonation depth and the logarithm of air-permeability coefficient. Computing the maximum relative difference for the square of carbonation depths, a maximum relative difference value of 57% is achieved. This difference is substantially higher than that obtained for air-permeability. Such difference is attributed to a decrease of the $Ca(OH)_2$ content, due to the pozzolanic action of SFCC, as experimentally confirmed by Zornoza et al. [10]. This means that besides an easier gas (CO_2) penetration, that is a physical mechanism, the increase in SFCC content also jeopardizes the chemical resistance to CO_2, as it causes some depletion of the alkaline reserve, allowing a further penetration of the carbonation front.

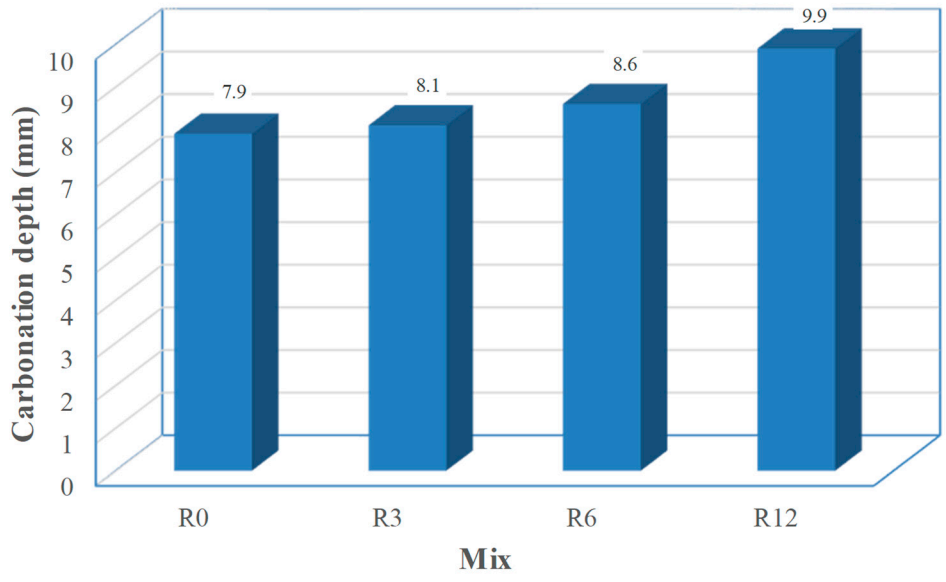

Figure 11. Carbonation depths.

3.6. Resistance to Chloride Penetration

The chloride ion penetrability of the mortar mixes is depicted in Figure 12. The resistance to chloride penetration improved as the replacement levels of cement by SFCC increased. Nevertheless, the chloride penetration in mixes R0 and R3 was quite similar and mix R6 exhibits just a slight decrease. The R12 mix presents a 17% decrease when compared with the reference mix (R0). Even though the assessed transport properties were found to increase with the SFCC content, the higher overall content of Al_2O_3 of this SCM provides higher chloride binding capacity [8]. According to Zornoza et al. [50], the improved binding capacity is due to the CAH and CASH compounds resulting from the pozzolanic reaction of SFCC. Then, the incorporation of untreated SFCC has two opposite effects regarding chloride resistance: on one hand, it facilitates the chloride transport; on the other hand, promotes the chemical bound of the coming chlorides, hindering the depth chloride penetration. These effects are quite balanced for mixes R3 and R6, while for the mix R12 the latter prevailed.

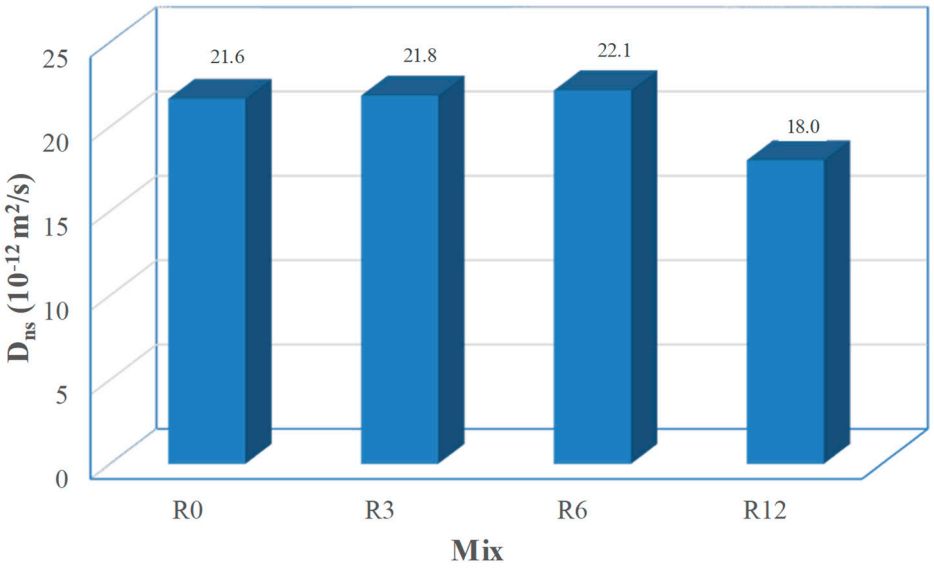

Figure 12. Non-steady state chloride diffusion coefficients (D_{ns}).

4. Conclusions

The influence of an as-received spent fluid cracking catalyst (SFCC), as cement replacement, on the performance of cement mortar was investigated.

It was found that the replacement of cement by SFCC, although untreated, is still able to improve the resistance to chloride penetration, while it has reduced the workability, the carbonation resistance, and compressive strength of mortar cured in standardized conditions. The transport properties (sorptivity and air-permeability) of mortar increased with the replacement of cement by untreated SFCC.

Finally, it was found that replacement of cement by SFCC had a positive effect on the compressive strength when curing in salt water.

Considering the previous findings, it is judged that untreated SFCC is a material suited for cementitious composites in marine applications, given its positive influence on the resistance to chloride penetration and on the compressive strength for saltwater curing. In fact, for such situations SFCC adds an interesting performance to environmental and economic benefits.

The use of superplasticizers to balance the found detrimental effects of SFCC incorporation, left outside the scope of the present investigation, is considered interesting and will be addressed in a forthcoming study.

Even though the untreated SFCC has jeopardized the resistance to the ingress of deleterious substances through the porous structure of the composite, as a supplementary cementing material

SFCC reduces the alkalinity of the pore solution and thus may be helpful regarding the mitigation of alkali–silica reaction. Therefore, it is highly recommended to study this issue in detail.

Author Contributions: Conceptualization, A.C. and B.S.d.F.; Methodology, A.C.; Validation, A.C.; Formal Analysis, B.S.d.F. and R.N.; Investigation, B.S.d.F.; Data Curation, R.D. and C.G.; Writing-Original Draft Preparation, B.S.d.F.; Writing-Review & Editing, R.N. and M.d.F.M.; Supervision, M.d.F.M.; Project Administration, A.C..

Funding: This research was funded by FCT—Fundação para a Ciência e Tecnologia grant number PTDC/ECM/105427/2008.

Acknowledgments: The authors are grateful to GALP Energia for providing the spent-zeolite, to SECIL for supplying the cement and to Betão Liz for supplying the aggregates.

Conflicts of Interest: The authors declare no conflict of interest.

References

1. Menezes, R.R.; Ferreira, H.S.; Neves, G.A.; Lira, H.D.L.; Ferreira, H.C. Use of granite sawing wastes in the production of ceramic bricks and tiles. *J. Eur. Ceram. Soc.* **2005**, *25*, 1149–1158. [CrossRef]
2. Pacewska, B.; Wilińska, I.; Kubissa, J. Use of spent catalyst from catalytic cracking in fluidized bed as a new concrete additive. *Thermochim. Acta* **1998**, *322*, 175–181. [CrossRef]
3. Su, N.; Fang, H.-Y.; Chen, Z.-H.; Liu, F.-S. Reuse of waste catalysts from petrochemical industries for cement substitution. *Cem. Concr. Res.* **2000**, *30*, 1773–1783. [CrossRef]
4. Neves, R.; Vicente, C.; Castela, A.; Montemor, M.F. Durability performance of concrete incorporating spent fluid cracking catalyst. *Cem. Concr. Compos.* **2015**, *55*, 308–314. [CrossRef]
5. Payá, J.; Monzó, J.; Borrachero, M.; Velázquez, S. Evaluation of the pozzolanic activity of fluid catalytic cracking catalyst residue (FC3R). Thermogravimetric analysis studies on FC3R-Portland cement pastes. *Cem. Concr. Res.* **2003**, *33*, 603–609. [CrossRef]
6. Zornoza, E.; Payá, J.; Monzó, J.; Borrachero, M.V.; Garcés, P. The carbonation of OPC mortars partially substituted with spent fluid catalytic catalyst (FC3R) and its influence on their mechanical properties. *Constr. Build. Mater.* **2009**, *23*, 1323–1328. [CrossRef]
7. Morozov, Y.; Castela, A.S.; Dias, A.P.S.; Montemor, M.F. Chloride-induced corrosion behavior of reinforcing steel in spent fluid cracking catalyst modified mortars. *Cem. Concr. Res.* **2013**, *47*, 1–7. [CrossRef]
8. Zornoza, E.; Payá, J.; Garcés, P. Chloride-induced corrosion of steel embedded in mortars containing fly ash and spent cracking catalyst. *Corros. Sci.* **2008**, *50*, 1567–1575. [CrossRef]
9. Pacewska, B.; Wilińska, I.; Bukowska, M.; Nocuń-Wczelik, W. Effect of waste aluminosilicate material on cement hydration and properties of cement mortars. *Cem. Concr. Res.* **2002**, *32*, 1823–1830. [CrossRef]
10. Zornoza, E.; Garcés, P.; Monzó, J.; Borrachero, M.V.; Payá, J. Accelerated carbonation of cement pastes partially substituted with fluid catalytic cracking catalyst residue (FC3R). *Cem. Concr. Compos.* **2009**, *31*, 134–138. [CrossRef]
11. Rodríguez, E.D.; Bernal, S.A.; Provis, J.L.; Gehman, J.D.; Monzó, J.M.; Payá, J.; Borrachero, M.V. Geopolymers based on spent catalyst residue from a fluid catalytic cracking (FCC) process. *Fuel* **2013**, *109*, 493–502. [CrossRef]
12. U.S. Geological Survey. Mineral Commodity Summaries—Cement. Available online: https://minerals.usgs.gov/minerals/pubs/commodity/cement/mcs-2018-cemen.pdf (accessed on 5 April 2018).
13. Alaejos, P.; Bermúdez, M. Influence of Seawater Curing in Standard and High-Strength Submerged Concrete. *J. Mater. Civ. Eng.* **2010**, *23*, 915–920. [CrossRef]
14. Comité Européen de Normalisation. *European Standard EN 197-1: Cement—Part 1: Composition, Specification and Conformity Criteria for Common Cements*; CEN: Brussels, Belgium, 2001.
15. Treacy, M.M.J.; Higgins, J.B. *Collection of Simulated XRD Powder Patterns for Zeolites*, 1st ed.; Elsevier: New York, NY, USA, 2001.
16. Luxan, M.P.; Madruga, F.; Saavedra, J. Rapid Evaluation Of Pozzolanic Activity Of Natural Products. *Cem. Concr. Res.* **1989**, *19*, 63–68. [CrossRef]
17. ASTM International. *ASTM C1437-15: Standard Test Method for Flow of Hydraulic Cement Mortar*; Annual Book of ASTM Standards; ASTM International: West Conshohocken, PA, USA, 2013. [CrossRef]

18. Comité Européen de Normalisation. *European Standard EN 196-1: Methods of Testing Cement—Part 1: Determination of Strength*; CEN: Brussels, Belgium, 2005.
19. ASTM International. *ASTM C1585-13: Standard Test Method for Measurement of Rate of Absorption of Water by Hydraulic-Cement Concretes*; Annual Book of ASTM Standards; ASTM International: West Conshohocken, PA, USA, 2013. [CrossRef]
20. SIA. *SN 505 262/1 Construction en Béton—Spécifications Complémentaires*; Annexe E: Perméabilité à L'air Dans les Structures Switzerland; SIA: Zurich, Switzerland, 2013.
21. Torrent, R. *Permea-TORR User Manual V1.2*; Materials Advanced Services: Buenos Aires, Argentina, 2009.
22. National Laboratory of Civil Engineering (LNEC). *E 391 Concrete: Determination of Carbonation Resistance*; Especificação E 391; LNEC: Lisbon, Portugal, 1993. (In Portuguese)
23. International Federation for Structural Concrete Task Group 5.6. Model Code for Service Life Design of Concrete Structures. In *Model Code for Service Life Design*; Schiessl, P., Ed.; International Federation for Structural Concrete (FIB): Lausanne, Switzerland, 2006.
24. NORDTEST. *Concrete, Mortar and Cement-Based Repair Materials: Chloride Migration Coefficient from Non-Steady State Migration Experiments*; NT Build 492; Proj. 1388-98; NORDTEST: Espoo, Finland, 1999; pp. 1–8.
25. ASTM International. *ASTM C1202-12: Standard Test Method for Electrical Indication of Concrete's Ability to Resist Chloride Ion Penetration*; Annual Book of ASTM Standards; ASTM International: West Conshohocken, PA, USA, 2012. [CrossRef]
26. Luping, T.; Nilsson, L.-O. Chloride diffusivity in high strength concrete at different ages. *Nord. Concr. Res.* **1992**, *11*, 162–171.
27. Chen, H.-L.; Tseng, Y.-S.; Hsu, K.-C. Spent FCC catalyst as a pozzolanic material for high-performance mortars. *Cem. Concr. Compos.* **2004**, *26*, 657–664. [CrossRef]
28. Su, N.; Chen, Z.-H.; Fang, H.-Y. Reuse of spent catalyst as fine aggregate in cement mortar. *Cem. Concr. Compos.* **2001**, *23*, 111–118. [CrossRef]
29. Zornoza, E.; Garcés, P.; Monzó, J.; Borrachero, M.V.; Payá, J. Compatibility of fluid catalytic cracking catalyst residue (FC3R) with various types of cement. *Adv. Cem. Res.* **2007**, *19*, 117–124. [CrossRef]
30. Payá, J.; Monzó, J.; Borrachero, M. Fluid catalytic cracking catalyst residue (FC3R): An excellent mineral by-product for improving early-strength development of cement mixtures. *Cem. Concr. Res.* **1999**, *29*, 1773–1779. [CrossRef]
31. Payá, J.; Monzó, J.; Borrachero, M.V.; Velázquez, S. Cement equivalence factor evaluations for fluid catalytic cracking catalyst residue. *Cem. Concr. Compos.* **2013**, *39*, 12–17. [CrossRef]
32. Tseng, Y.-S.; Huang, C.-L.; Hsu, K.-C. The pozzolanic activity of a calcined waste FCC catalyst and its effect on the compressive strength of cementitious materials. *Cem. Concr. Res.* **2005**, *35*, 782–787. [CrossRef]
33. Taylor, H.F.W. *Cement Chemistry*, 2nd ed.; Thomas Telford: London, UK, 1997.
34. Hewlett, P.C. *Lea's Chemistry of Cement and Concrete*; Elsevier Butterworth-Heinmann: Amsterdam, The Netherlands, 2004.
35. Akinkurolere, O.O.; Jiang, C.; Shobola, O.M. The influence of salt water on the compressive strength of concrete. *J. Eng. Appl. Sci.* **2007**, *2*, 412–415.
36. Griffin, D.F.; Henry, R.L. *The Effect of Salt in Concrete on Compressive Strength, Water Vapour Transmission and Corrosion of Reinforcing Steel*; Naval Civil Engineering Lab: Port Hueneme, CA, USA, 1964.
37. Maniyal, S.; Patil, A. An Experimental Study on Compressive Strength of Various Cement Concrete Under Sea Water. *Int. J. Sci. Eng. Res.* **2015**, *6*, 199–203.
38. Wegian, F.M. Effect of seawater for mixing and curing on structural concrete. *IES J. Part A Civ. Struct. Eng.* **2010**, *3*, 235–243. [CrossRef]
39. Bai, J.; Wild, S.; Sabir, B.B. Chloride ingress and strength loss in concrete with different PC–PFA–MK binder compositions exposed to synthetic seawater. *Cem. Concr. Res.* **2003**, *33*, 353–362. [CrossRef]
40. Kumar, S. Influence of water quality on the strength of plain and blended cement concretes in marine environments. *Cem. Concr. Res.* **2000**, *30*, 345–350. [CrossRef]
41. Kropp, J.; Alexander, M. Transport mechanisms and reference tests. In *Non-Destructive Evaluation of the Penetrability and Thickness of the Concrete Cover*; Torrent, R., Luco, L.F., Eds.; RILEM Publications SARL: Paris, France, 2007; pp. 13–34.
42. Garboczi, E.J.; Bentz, D.P. Modelling of the microstructure and transport properties of concrete. *Constr. Build. Mater.* **1996**, *10*, 293–300. [CrossRef]

43. Mehta, P.K.; Monteiro, P.J.M. *Concrete: Microstructure, Properties, and Materials*; McGraw-Hill Education: New York, NY, USA, 2006.
44. Barbhuiya, S.A.; Gbagbo, J.K.; Russell, M.I.; Basheer, P.A.M. Properties of fly ash concrete modified with hydrated lime and silica fume. *Constr. Build. Mater.* **2009**, *23*, 3233–3239. [CrossRef]
45. Yüksel, C.; Mardani-Aghabaglou, A.; Beglarigale, A.; Yazıcı, H.; Ramyar, K.; Andiç-Çakır, Ö. Influence of water/powder ratio and powder type on alkali–silica reactivity and transport properties of self-consolidating concrete. *Mater. Struct.* **2016**, *49*, 289–299. [CrossRef]
46. Comité Européen de Normalisation. *European Standard EN 1504-3: Products and Systems for the Protection and Repair of Concrete Structures—Definitions, Requirements, Quality Control and Evaluation of Conformity*; CEN: Brussels, Belgium, 2005.
47. Neves, R.; Branco, F.; de Brito, J. About the statistical interpretation of air permeability assessment results. *Mater. Struct.* **2012**, *45*, 529–539. [CrossRef]
48. Torrent, R.; Frenzer, G. *Methoden zur Messung und Beurteilung der Kennwerte des Uberdeckungsbetons auf der Baustelle—Teil 2*; Office Federal des Routes: Bern, Switzerland, 1995.
49. Hilsdorf, H.K. Durability of concrete—A measurable quantity? In Proceedings of the IABSE Symposium, Lisbon, Portugal, 6–8 September 1989; IABSE-AIPC-IVBH: Zurich, Switzerland, 1989; pp. 111–123.
50. Zornoza, E.; Garcés, P.; Payá, J.; Climent, M.A. Improvement of the chloride ingress resistance of OPC mortars by using spent cracking catalyst. *Cem. Concr. Res.* **2009**, *39*, 126–139. [CrossRef]